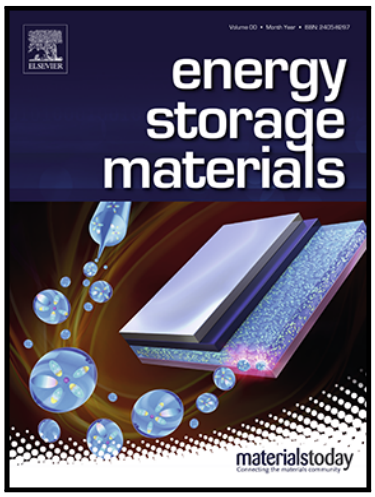

Achieving ultra-long lifespan Zn metal anodes by manipulating desolvation effect and Zn deposition orientation in a multiple cross-linked hydrogel electrolyte

Pengxiang Lin , Jianlong Cong , Jiyang Li , Minghao Zhang , Pengbin Lai , Jing Zeng , Yang Yang , Jinbao Zhao

PII: S2405-8297(22)00200-8
DOI: https://doi.org/10.1016/j.ensm.2022.04.010
Reference: ENSM 2186

To appear in: *Energy Storage Materials*

Received date: 13 December 2021
Revised date: 29 March 2022
Accepted date: 5 April 2022

Please cite this article as: Pengxiang Lin , Jianlong Cong , Jiyang Li , Minghao Zhang , Pengbin Lai , Jing Zeng , Yang Yang , Jinbao Zhao , Achieving ultra-long lifespan Zn metal anodes by manipulating desolvation effect and Zn deposition orientation in a multiple cross-linked hydrogel electrolyte, *Energy Storage Materials* (2022), doi: https://doi.org/10.1016/j.ensm.2022.04.010

Pengxiang Lin, Jianlong Cong, Jiyang Li, Minghao Zhang, Pengbin Lai, Jing Zeng, Yang Yang, * Jinbao Zhao *

College of Chemistry and Chemical Engineering, State-Province Joint Engineering Laboratory of Power Source Technology for New Energy Vehicle, State Key Laboratory of Physical Chemistry of Solid Surfaces, Engineering Research Center of Electrochemical Technology, Ministry of Education, Collaborative Innovation Center of Chemistry for Energy Materials, Xiamen University, Xiamen, 361005, PR China

AUTHOR INFORMATION

Corresponding Author

*Professor Jinbao Zhao, College of Chemistry & Chemical Engineering, Xiamen university

Xiamen university

Xiamen 361005

China, Email: yangyang419@xmu.edu.cn (Yang Yang); jbzhao@xmu.edu.cn (Jinbao Zhao).

Achieving ultra-long lifespan Zn metal anodes by manipulating desolvation effect and Zn deposition orientation in a multiple cross-linked hydrogel electrolyte

Highlights

1. An ultra-long cycle life of 5000 h with a high coulombic efficiency of 99.5%;
2. Reducing the desolvation energy barrier (62.31 kJ mol^{-1} to 36.42 kJ mol^{-1});
3. Guiding the preferential orientation of Zn deposition simultaneously;
4. Use a simple one-pot synthesizing method.

Abstract

Aqueous zinc-ion batteries (ZIBs) have received extensive attention due to the intrinsic advantages of high safety, low cost and environmental friendliness. But detrimental side reactions and dendrite problems resulting from high desolvation penalty and inhomogeneous Zn^{2+} flux at the interface severely hindered their practical applications. Herein, a novel polyacrylamide-poly (ethylene glycol) diacrylate-carboxymethyl cellulose (PMC) hydrogel electrolyte is designed to overcome these obstacles through reducing the desolvation energy barrier and guiding the preferential orientation of Zn deposition simultaneously. Theoretical calculation and experimental results reveal that the desolvation activation energy of the PMC hydrogel electrolyte (36.42 kJ mol^{-1}) is substantially lower than that of conventional $ZnSO_4$ aqueous electrolyte (62.31 kJ mol^{-1}) due to the regulated Zn^{2+} solvation structure. Based on the high binding energy between amide groups and Zn^{2+}, polymer chains in PMC also serve as facile Zn^{2+} transport channels to guide the uniform deposition behavior on the Zn (002) crystal surface, which is verified by the grazing incidence XRD analysis. Consequently, an ultra-long cycle life of 5000 h with a high coulombic efficiency of 99.5% is achieved by using the PMC hydrogel electrolyte. Considering the simple one-pot synthesizing method, the PMC hydrogel electrolyte provides new opportunities for developing practical ZIBs.

Keywords: zinc ion battery, multiple cross-linked hydrogel electrolyte, ultra-long lifespan, desolvation effect, preferred orientation deposition

1. Introduction

With the vast consumption of fossil energy and the severe environmental pollution, the demand for low-cost and sustainable clean energy has been increasing rapidly. Because of the high energy density and excellent cycling stability, lithium-ion batteries (LIBs) have been widely used in portable devices and electric vehicles. However, the potential safety issues and high cost of LIBs have restricted their application in large-scale energy storage fields.[1-4] Due to the relatively high specific capacity of zinc metal (820 mAh g^{-1}) and the non-flammability of aqueous electrolytes, aqueous zinc-ion batteries (AZIBs) bring many unique benefits over commercial LIBs to be worthy of being considered as promising candidates for large-scale electrochemical energy storage applications.[5-7] Nowadays, the most commonly-used electrolyte in the AZIBs is zinc sulfate. However, it would result in the poor cycle stability and low coulombic efficiency of zinc anodes, which can be attributed to the following two reasons: i) the increased internal resistance caused by the generation of by-products (the generation of $Zn_4(OH)_6SO_4 \cdot xH_2O$);[8-10] ii) the internal short circuit caused by zinc dendrites formed disorderly on the anode surface.[11, 12] These problems have seriously hindered the practical application of AZIBs.[8, 9, 13, 14]

So far, many efforts have been made to improve the electrochemical performance of Zn metal anodes, such as alloying of zinc metal,[15, 16] surface coating[11, 17-19], high-concentration electrolyte, and electrolyte additives[20-23]. In addition to these commonly-used strategies, designing hydrogel electrolytes to replace traditional

aqueous electrolytes has been also proved to be effective in restraining Zn dendrite growth and side reactions.[24-26] These designs include: 1. Tuning ions flux and inducing uniform deposition in the interface[24, 27, 28]; 2. Restricting the Two-dimensional diffusion of zinc ions by electrostatic interactions and functionalized groups; [12, 27] 3.Reducing the activity of water molecules by restricting its movement in gel toward suppressing the side reactions.[29] Besides, the quasi-solid hydrogel electrolyte formed by polymer has high stability and certain flexibility, which is also suitable for assembling flexible aqueous zinc ion batteries (FAZIBs). In practical applications, benefit from the superior mechanical strength , the flexible zinc-ion batteries have better resistance to the external impact and damage than traditional aqueous zinc-ion batteries.[30-32] At present, it has a wide range of application prospects in smart wear,[31] biological implantable electronic devices,[33] and extreme environments.[34, 35] Despite the great progress, two underlying points usually has not been paid enough attention for the development of high-performance hydrogel electrolytes for AZIBs. One is that the desolvation process of $[Zn(H_2O)_6]^{2+}$ consumes a huge amount of energy with zinc deposition in an aqueous electrolyte, which may trigger hydrogen evolution reaction (HER). This will increase the pH value at the reaction interface and lead to the formation of by-products ($Zn_4(OH)_6SO_4 \cdot xH_2O$). The electronic insulation and non-electroactive properties of the by-products will further increase the uneven distribution of the electric field on the surface of the negative electrode. Although HER can be to some extent reduced due to the decrease of water activity in the hydrogel electrolyte, the

desolvation pentalty still remains formidable. The other crucial factor that should be carefully considered is the crystal orientation of deposition Zn, which is closely associated with dendrite growth. Typically, metallic Zn tends to grow along the (101) plane, that is mostly prone to the formation of vertical Zn dendrites. Recent studies indicate that the binding energy of zinc on the (002) crystal plane is much lower than that on the (101) crystal plane, which is more resistant to the formation of dendrite than the Zn(100) and Zn(101) crystal planes.[36] Accordingly, various interface modification approaches such as introducing graphene coating layer and using more (002) basal plane texture exposed Zn foil have been adopted to affect the crystal orientation of deposition Zn.[7, 37] However, how to guide the (002) crystal plane preferred Zn plating/stripping behavior in the hydrogel electrolyte is rarely involved. Therefore, it is of a great challenge to develop a novel hydrogel electrolyte that can reduce the activation energy of desolvation and guide the deposition of zinc ions on the Zn (002) crystal surface simultaneously.

Herein, we designed a simple one-pot method to prepare a hydrogel electrolyte PAM-PEGDA-CMC (PMC) with the ability to reduce the activation energy of desolvation process, and guide the preferential orientation of zinc ions deposition. In a rational design, the free radicals generated by APS through thermally initiated, which allow the polymerization of acrylamide (AM) monomers and poly(ethylene glycol) diacrylate (PEGDA) as a cross-linking agent to generate covalent bonds , and finally bridge to form the basic structure of the 3D network.[38, 39]The carboxymethyl cellulose (CMC) molecular chains shuttle through the 3D network to form a

semi-interpenetrating network (Figure Sx).[40, 41] Through electrochemical impedance spectroscopy (EIS) and grazing incidence XRD (GIXRD) analysis, it is found that the amide group of the PAM molecule in the formed 3D hydrogel plays a key role in reducing the desolvation activation energy and achieving the dendritic-free and highly prefer orientation deposition/stripping of the zinc anode. The symmetric Zn/Zn battery assembled by the PMC electrolyte has an ultra-long cycle time (~5000 h), and the Zn/Cu half-battery has highly reversible Zn deposition/exfoliation (99.5% average Coulomb efficiency). Meanwhile, the flexible battery assembled using PMC hydrogel electrolyte shows excellent safety and durable, which can still work normally under the harsh conditions of punching and bending.

2. Results

Synthesis and characterization of materials

The method of synthesis PMC hydrogel electrolyte is shown in Figure 1a. AM, PEGDA, CMC and APS were completely dissolved in 2.0 M $ZnSO_4$ solution to obtain a clear and transparent solution. The mixture was poured into the template and heated to 40 °C on the heating plate. During the heating process, free radicals released from APS acted on the carbon-carbon double bond and initiated the polymerization. Constant temperature for 30 min and cooled down to room temperature to obtain PMC hydrogel electrolyte. As shown in Figure 1b, the hydrogel electrolyte is colorless and transparent. The thickness of the PMC hydrogel electrolyte controlled by the mold is almost the same as the commercially available glass fiber (Figure S2). This makes that the thickness of the battery assembled in the subsequent experiment

is the same and ensures the accuracy of the experiment. At the same time, we found that PMC has good flexibility (Figure S3), which shows that the gel has the prospect in flexible batteries. The tensile strengths of pure PAM gel, PAM-PEGDA and PAM-PEGDA-CMC (PMC) were measured by an electronic tensile testing machine (Figure 1d). It is found that after adding the PEGDA (the cross-linking agent), PAM and PEGDA polymerize to form a 3D structure, which increase the tensile strength of the hydrogel. Furthermore, after adding CMC, the tensile strength of the hydrogel is further improved significantly. This is because CMC and PAM-PEGDA form a semi-interpenetrating three-dimensional network structure, which further increases the mechanical properties of the hydrogel.[42, 43] The tensile strength of the PMC gel electrolyte reached 2.25 MPa. Symmetric batteries were assembled with PMC as the electrolyte, and cycled for 0, 20, and 50 hours, and then disassembled to find that the PMC gel remained intact (Figure S4). This shows that the excellent mechanical properties of PMC can keep it stable during cycling. As shown in Figure 1c, the Fourier transform infrared spectroscopy analysis of PMC in different states, tells that there is no obvious characteristic peak of C=C bond (purple area) in PMC, which indicates that PMC is a covalent cross-linking induced by free radicals obtained by polymerization. The dark green area represents the characteristic peak of zinc sulfate. The light green area is the characteristic peak of Zn-O bond. In order to further prove the reliability of the Zn-O bond, we also performed the XPS test on the PMC. It can be seen from Figure S5 that there are obvious characteristic peaks of the Zn-O bond in the Zn2p analysis pattern.[44] The corresponding characteristic peaks of Zn-O bonds

can also be fitted in the O1s spectrum. The PMC hydrogel electrolyte was dried in an oven at 80 °C, and the water content (free water) was 63.97%. The PMC gel electrolyte was frozen in liquid nitrogen to obtain a relatively flat section. After drying the moisture, scanning electron microscope (SEM) images and Zn EDS element map show that the zinc element is evenly distributed in the PMC hydrogel electrolyte (Figure S6 a&b).

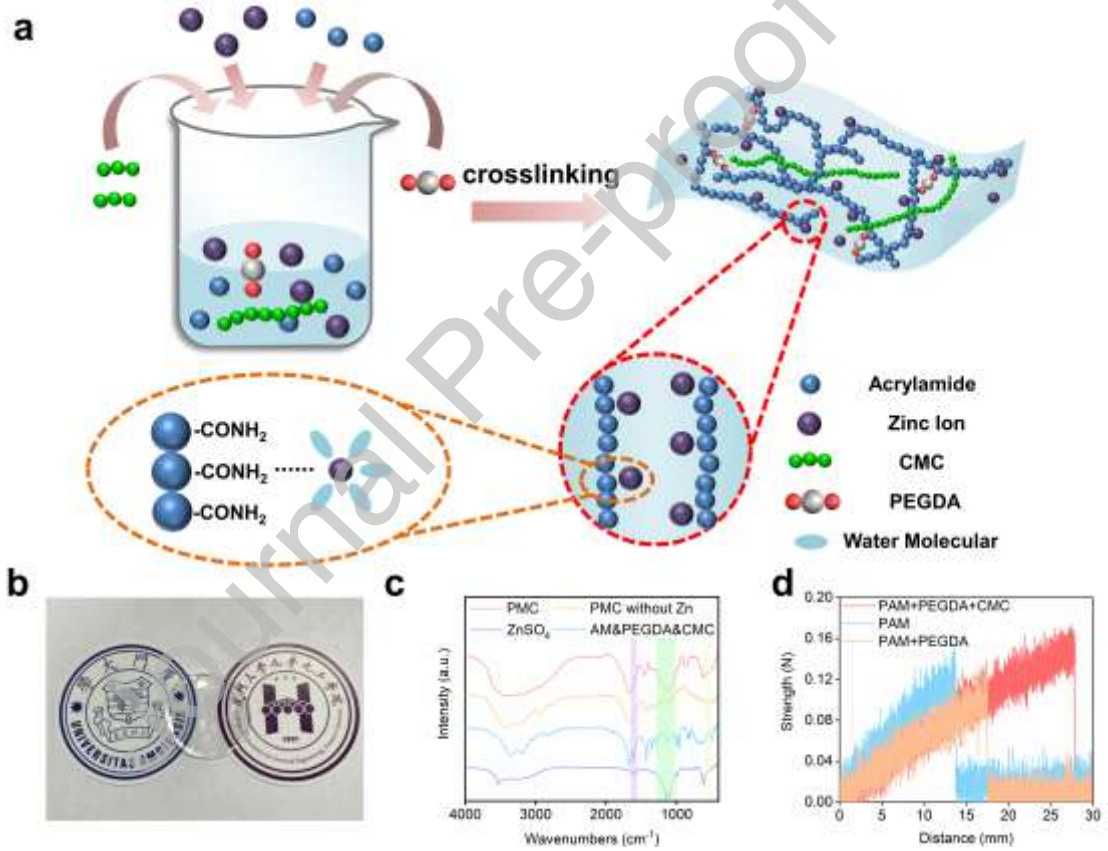

Fig 1. Synthesis and characterization of PMC gel electrolyte. (a) Synthetic schematic diagram of PMC hydrogel electrolyte; (b) Optical photograph of PMC hydrogel electrolyte; (c) Infrared image of PMC hydrogel electrolyte; (d) Tensile strength test (PAM+PEGDA+CMC, PAM and PAM+PEGDA).

Electrochemical performance

Next, the electrochemical properties of PMC were verified. We used stainless steel foil as the working electrode, zinc foil as the counter electrode and reference electrode. The data obtained by linear scanning voltammetry (LSV) is shown in Figure 2a. This result indicates that PMC gel electrolyte has a high electrochemical stability window of ~2.2V (vs. Zn/Zn^{2+}), which can satisfy the needs of AZIBs. In order to study the ionic conductivity of PMC hydrogel and AM-PEGDA-CMC aqueous solution, we characterized the ionic conductivity by EIS. As shown in Figure 2b, the ionic conductivity of the aqueous solution before polymerization is calculated by formula (1) to be 35.71 mS cm^{-1}. The ionic conductivity of the PMC gel electrolyte is 30.24 mS cm^{-1}. This indicates that the polymerization has a litter effect on the ionic conductivity, but it is still superior to the most of present research (Table S1). [28, 35, 45-47] The zinc foil was cut into a square of 5 mm*5 mm and used as the working electrode and the counter electrode in the three-electrode cell, while the reference electrode was saturated calomel electrode (SCE). Here, we use a three-electrode electrolytic cell to test the Tafel curves of different electrolytes to analyze the influence on the corrosion of the zinc foil. (Figure 2c). Compared with the 2.0 M $ZnSO_4$ solution, it can be seen that the corrosion potential of zinc foil in PMC rises from -1.025 V to -0.995 V, which means zinc foil is hard to be corroded in PMC. The corrosion current of PMC hydrogel electrolyte ($0.798*10^{-3}$ mA cm^{-2}) is weaker than that of $ZnSO_4$ electrolyte ($1.226*10^{-3}$ mA cm^{-2}), indicating that PMC hydrogel electrolyte has less corrosion on zinc foil than $ZnSO_4$. Therefore, PMC hydrogel is

suitable as an electrolyte for zinc ion batteries. The symmetric Zn/Zn batteries were tested to estimate the cycling stability of the PMC hydrogel electrolyte. As shown in Figure 2d, the symmetrical battery assembled with PMC hydrogel electrolyte exhibits great cycling stability, for nearly 5000 h at a current density of 1.0 mA cm^{-2} and a capacity density of 1.0 mAh cm^{-2}. In contrast, the symmetrical battery assembled with the 2.0 M $ZnSO_4$ aqueous electrolyte shows an increasing polarization around 150 h, and short circuit around 160 h. At the same time, we studied the cycle performance of symmetrical battery under different current density and capacity density. All of the Zn/PMC/Zn batteries exhibits terrific cycle stability (Figure S7). However, in the symmetric Zn/Zn batteries where AM-PEGDA-CMC served as the additive, short-circuits happened only after a stable cycle of ~2500 h. This tells us that the polymerized PMC hydrogel electrolyte has a better optimization effect on the Zn anode during cycling. Moreover, the cycle voltage of the Zn/Zn symmetric battery (effective zinc foil area is 1.13 cm^2) remains stable at a current of 0.2-20.0 mA (Figure S8), and the polarization voltage has been stable around ~80 mV. The copper foil with10.0 mAh cm^{-2} of Zn predeposited is also used as the test electrode with a limited content of Zn for the deep charge/discharge. It can cycle for more than 400 h at a current density of 1.0 mA cm^{-2} and capacity density of 2.0 mAh cm^{-2} (corresponding to the DOD of 20%, Figure S9). This indicates that the PMC hydrogel electrolyte not only has an ultra-stable cycle life, but also can be used as the electrolyte for zinc-ion batteries in a wide range of current density. The PMC hydrogel electrolyte provides a more stable cycle compared with other symmetrical

batteries in the same period (Figure 2e).

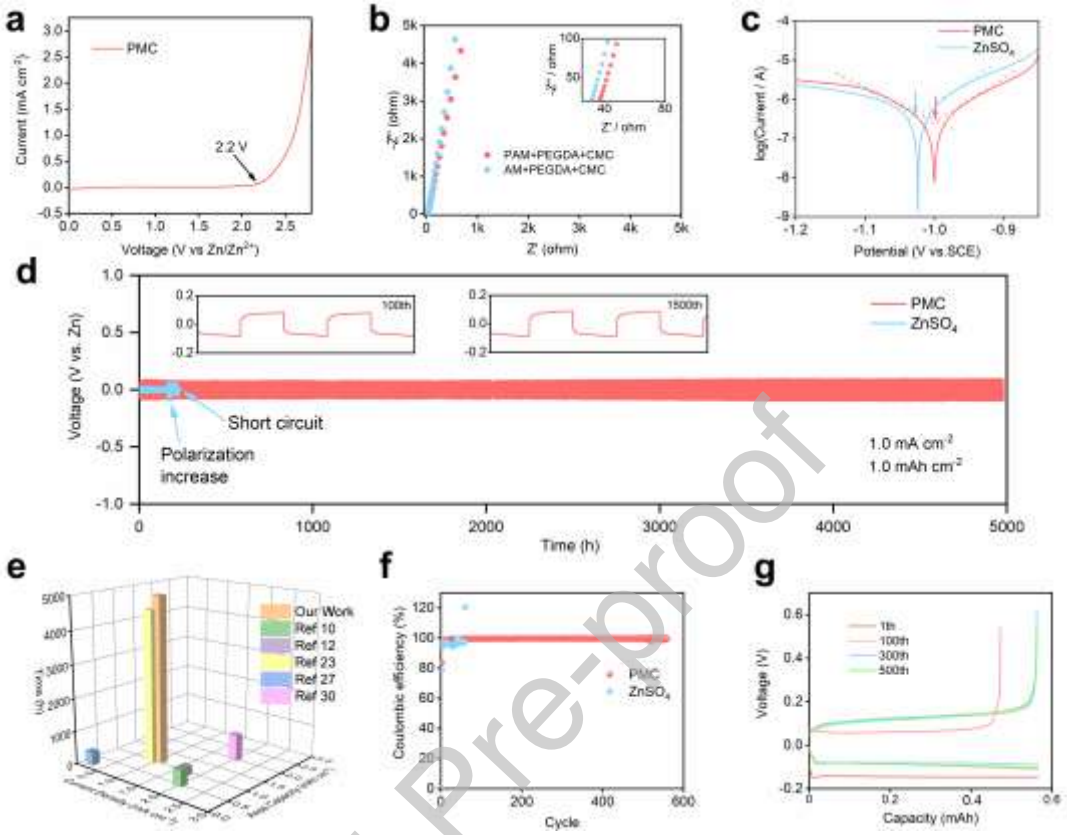

Fig 2. Electrochemical performance of PMC hydrogel electrolyte. (a) The PMC hydrogel electrolyte's electrochemical window; (b) EIS spectra of polymerized hydrogel and non-polymerized hydrogel, the inset is an enlarged view of the low frequency region; (c) Tafel curve of PMC gel electrolyte and 2.0 M $ZnSO_4$ electrolyte; (d) The cycle voltage curves of Zn/Zn symmetric batteries with different electrolytes, the illustrations are the 100th cycle and 1500 cycles respectively; (e) Compared with the Zn/Zn symmetric battery in the reported work; (f) The cycle performance of Zn/Cu asymmetric battery assembled with PMC or 2.0 M $ZnSO_4$; (g) PMC as the Zn/Cu asymmetric battery Electrolyte voltage/capacity graph.

For batteries, reversibility is also very important. Here we assemble a Zn/Cu asymmetric battery, using respectively PMC or 2.0 M $ZnSO_4$ as electrolytes. They are used to verify the contribution of PMC hydrogel electrolyte to the cycle reversibility of Zn deposition/exfoliation. As shown in Figure 2f, the coulombic efficiency of the battery assembled with PMC gel electrolyte is stable more than 500 cycles. The first lap coulombic efficiency is as high as 83.7%, and the average coulombic efficiency is 99.5%. In comparison, the first cycle Coulomb efficiency of the battery assembled with $ZnSO_4$ electrolyte is only 79.0%, and the short circuit occurs less than 60 cycles. The voltage/capacitance graphs of different cycles (Figure 2g) also show that the Zn/Cu asymmetric battery using PMC hydrogel as the electrolyte can maintain a low overpotential to ensure stable long-term cycles. All these indicate that the hydrogel can effectively inhibit the side reactions that occur during zinc deposition/exfoliation in Zn/Cu asymmetric battery cycling.

Mechanism derivation

In order to explore the long-term and stable circulation mechanism of PMC hydrogel electrolyte. First of all, we used PMC and 2.0 M $ZnSO_4$ as electrolytes to assemble Zn/Zn symmetrical batteries to cycle (current density: 1.0 mA cm^{-2}, capacity density: 1.0 mAh cm^{-2}) for different periods of time. Carried out the Zn foils and imaged by SEM. As shown in Figure 3, compared with the zinc foil that has not been cycled (Figure S10), after cycles of 100 h the symmetrical battery assembled with PMC hydrogel electrolyte has a regular deposition morphology (Figures 3a and S11a).

The surface of the zinc foil after the 200 h of cycles still maintains a uniform appearance (Figure 3c and S11b). The symmetrical battery assembled with $ZnSO_4$ aqueous electrolyte solution shows scaly dendrites and by-products after 100 h cycles (Figure 3b), and more dendrites and by-products appeared on the surface when the cycle continued to 200 h (Figure 3d). Shape-measuring laser microscope is used to image the zinc foils after cycling with different electrolytes. As shown in Figure S12, the Zn foils cycled with PMC as electrolyte exhibited similar flatness to the pristine Zn foils, while which assembled with $ZnSO_4$ as the electrolyte become very rough. In addition, more intuitive evidence can be seen under the in-situ optical microscope. It can be seen from Figure 3e that in the battery assembled with PMC hydrogel electrolyte, the cross-section of zinc foil appears uniform and dense deposition. On the contrary, the battery assembled with 2.0 M $ZnSO_4$ aqueous electrolyte appears small protrusions after 10 minutes, and gradually evolved into dendrites over time. These phenomena show that the PMC hydrogel electrolyte can not only inhibit the occurrence of by-reactions during Zn deposition/exfoliation, but also make Zn uniformly deposited on the surface of the zinc foil.

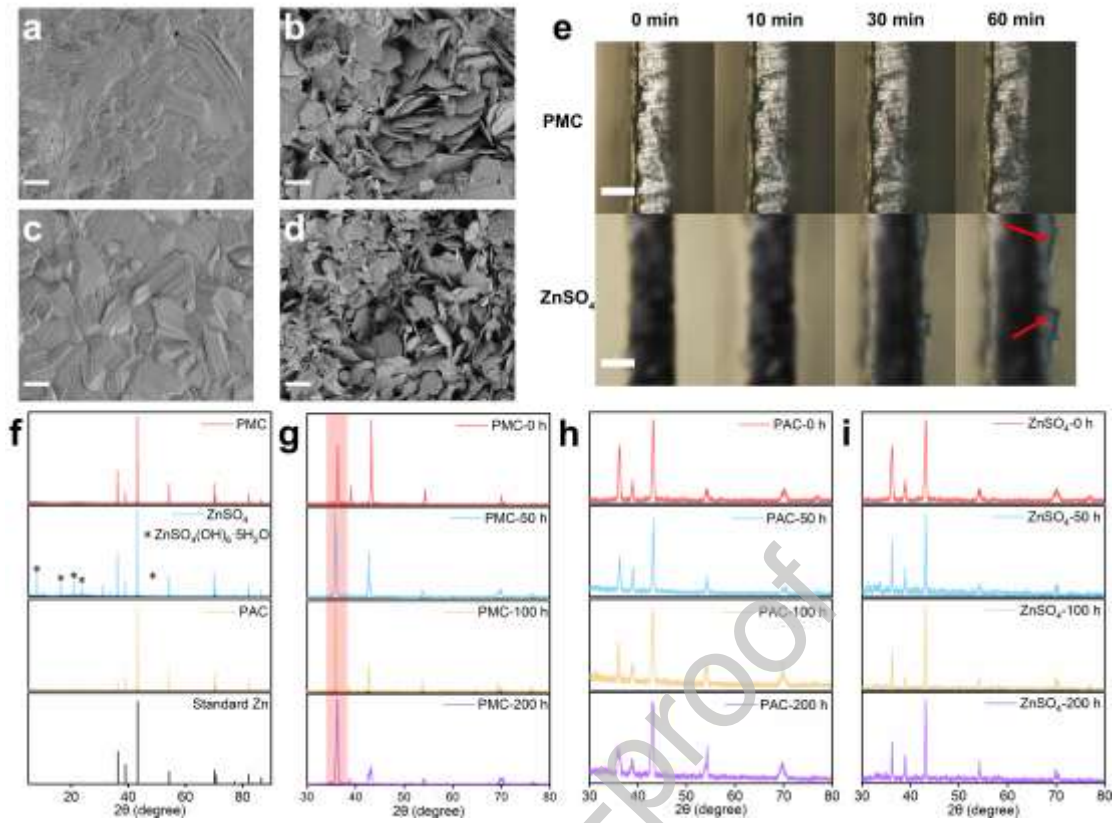

Fig 3. The influence of PMC hydrogel electrolyte on the deposition/exfoliation of zinc anode. SEM image of zinc foil surface after cycling of (a) 100 h and (c) 200 h; SEM image of zinc foil surface after cycling (b) 100 h (d) 200 h; (e) The deposition morphology of the cross-section of zinc foil at different times captured by in-situ optical microscope (electrolyte: PMC hydrogel and 2.0 M $ZnSO_4$ aqueous solution, current density: 5.0 mA cm^{-2}). The scale bar in (a), (b), (c), (d) is 10 μm. The scale bar in (e) is 800 μm. (f) XRD pattern of Zn foil after 50 h cycle of Zn/Zn symmetric battery assembled with different electrolytes; GIXRD diffraction patterns of Zn/Zn symmetric batteries assembled with different electrolytes after cycling for 50 h, 100 h, and 200 h (g) PMC, (h) PAC, (i) $ZnSO_4$; (current density: 1.0 mA cm^{-2}; capacity density: 1.0 mAh cm^{-2});

Here we speculate that the reason for the different deposition forms from PMC hydrogel electrolyte to $ZnSO_4$ aqueous solution electrolyte is that the zinc ion channel formed by the amide group in polyacrylamide can guide the uniform deposition of zinc ions.[24, 36] This is because PAM has a strong absorption of polar zinc and the binding energy is -1.25 eV is much higher than the zinc surface.[20] When PMC is used as a hydrogel electrolyte, a large number of amide groups on the polymer chain can guide continuous zinc transmission, so that zinc can be uniformly transported to the surface of the anode. In order to verify the influence of the amide group in the PMC hydrogel electrolyte on the zinc deposition, we first used X-ray diffraction (XRD) to characterize the zinc foil in the Zn/Zn symmetric batteries with PMC, 2.0 M $ZnSO_4$ and PAC (acrylic acid as monomer, the polymer does not contain amide) electrolytes after 50 h cycles. As shown in Figure 3f, a large amount of double hydroxide (LDH) $Zn_4SO_4(OH)_6{\cdot}5H_2O$ (JCPDS NO: 39-0688) appeared on the surface of the zinc foil after cycling the Zn/Zn symmetric battery using the 2.0 M $ZnSO_4$ aqueous solution electrolyte:

$$4Zn^{2+}+6OH^-+SO_4^{2-}+5H_2O\rightarrow Zn_4(OH)_6SO_4{\cdot}5H_2O \qquad (1)[24]$$

However, the Zn/Zn symmetric battery using PMC hydrogel electrolyte has no other obvious diffraction peaks except for the characteristic diffraction peak of zinc, which further shows that PMC hydrogel electrolyte can effectively inhibit the occurrence of by-reactions.

In order to eliminate the interference of the substrate on the exploration, we performed grazing incidence X-ray diffraction (GIXRD) to analyze the changes in the

crystal structure of the zinc foil surface in the cycle of the Zn/Zn symmetric battery assembled with PMC hydrogel electrolyte for different periods of time. As shown in Figure 3g, with the increase of cycle time, the diffraction peaks of (002) crystal planes (red area) become stronger, while the diffraction peaks of (101) crystal planes become weaker, indicating that the PMC gel electrolyte could guide the deposition orientation in witch lower Zn^{2+} tends to follow the direction of the (002) crystal plane. In order to verify that the preferred orientation of zinc deposition is the guiding effect of the amide group, we not only performed GIXRD characterization on the zinc foil after cycling the symmetric battery assembled with $ZnSO_4$ (Figure 3i), but also synthesized the PAC hydrogel by changing the monomer from AM to AA (AA without amide group). The PAC hydrogel is used as the electrolyte to assemble a Zn/Zn symmetric battery after different cycles of time, and the zinc foil is characterized by GIXRD, as shown in Figure 3h. The results show that the zinc foil of the Zn/Zn symmetric battery assembled by the PAC hydrogel electrolyte has no change in the crystal plane of the surface after cycling for different time. Which further shows that the PMC hydrogel electrolyte we synthesized has the function of guiding the deposition of zinc in the preferred orientation. It is because the zinc ion channel formed by the amide group in the molecule plays a key role.

In the $ZnSO_4$ solutions, zinc ions exist as the form of hexahydrate ($[Zn(H_2O)_6]^{2+}$), so a large amount of energy provided for the desolvation process when depositing at the interface of the zinc foil, which is easily to beget hydrogen evolution reactions (HER).[48-50] And the local pH reduction at the interface caused by the HER will be

accompanied by the production of by-products on the surface of the zinc foil. Therefore, if the $[Zn(H_2O)_6]^{2+}$ can be desolvated in advance, the by-products produced during the cycle of the zinc anode will be reduced the production of the product. The desolvation process of Zn^{2+} is usually the rate-limiting step of the anode zinc deposition, it can be expressed by the activation energy (Ea) of the Arrhenius equation:

$$\frac{1}{R_{ct}} = Ae^{-(E_a/RT)} \quad (2)\ [49, 51]$$

Where Rct is the interface resistance, A is the frequency factor, R is the gas constant, and T is the absolute temperature. PMC's ability to inhibit side reactions may be due to the fact that the strong polar amide group in PMC is easy to bond with zinc ions, which helps to remove the solvating sheath of zinc hexahydrate ions during the cycle. In order to verify this phenomenon, we investigate the changes of desolvation energy in PMC and $ZnSO_4$ through variable temperature EIS. It can be seen from Figures 4a and b that the Rct (1056.0) of Zn foil in $ZnSO_4$ solution at 303.15 K is significantly higher than that of PMC (830.0), which confirms the improvement of the charge transfer ability in PMC (Table S2). From Figure 4c, we can see that the Ea in PMC is about 36.42 kJ mol^{-1}, while the Ea in $ZnSO_4$ is 62.31 kJ mol^{-1}. This indicates that the strong polar amide group in PMC has a positive effect on the Zn^{2+} desolvation sheath.

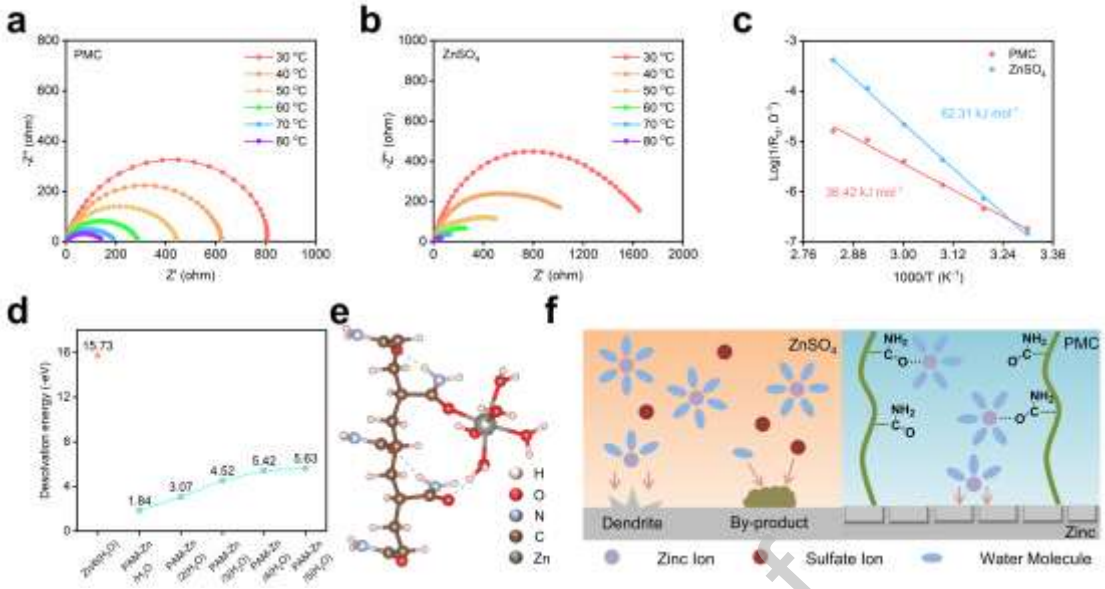

Fig 4. The mechanism of PMC hydrogel electrolyte guiding the uniform deposition of zinc. The variable temperature EIS of (a)PMC and (b)$ZnSO_4$; (c) The calculated desolvation activation energies of both electrolyte by using the Arrhenius equation. (d) Simulates the desolvation energy of zinc ions in the solvation sheath with different water content; (e) Molecular model simulation diagram of PAM-Zn/5H_2O; (f) The deposition/exfoliation mechanism of Zn^{2+} on the surface of Zn foil in $ZnSO_4$ aqueous electrolyte and PMC hydrogel electrolyte.

In conventional liquid electrolytes, solvated ions are transported simultaneously with the solvation sheath. However, the solvation sites are fixed in solid electrolyte, where the ions are transported through coupling-dissociation processes or frequent exchange of mobile solvent molecules, and the two types of ion transport modes can be run in parallel.[52-55] The property of gel electrolyte is between the liquid electrolyte and solid electrolyte, so its ion transport mode is also between the two kinds of electrolyte. Through the work of Wang et al., it was found that the binding energy of the amide

group to the zinc ion is very low.[20] Combined with our calculations, it is found that the oxygen atoms on the amide group are more likely to bind Zn ions (Figure S13). Therefore, we believe that PMC has the ability to bind with hydrated zinc ions to guide the deposition of zinc ions and reduce the desolvation energy during deposition. At the anode interface of Zn-ion batteries, the deposition/stripping of zinc is three consecutive steps: 1). The movement of hydrated zinc ions from the electrolyte toward the surface of the anode; 2) The desolvation of hydrated zinc ions at the interface; 3). The redox reaction of zinc ions or zinc on the surface of the anode occurs. And it is generally accepted that the desolvation process is the rate determined step during the whole charge-transfer process.[49, 50] For the $ZnSO_4$ aqueous electrolyte, the desolvation process at the interface is:

$$Zn(H_2O)_6^{2+} \rightarrow Zn + 6H_2O \quad (3)$$

For the PMC hydrogel electrolyte, the redox reaction at the anode interface is:

$$PMC\text{-}Zn(H_2O)_x^{2+} \rightarrow Zn + xH_2O \ (1 \leq x \leq 5) \quad (4)$$

As described in Figure 4d in the manuscript, we calculated the desolvation energie of hydrated zinc ions that lose varying amounts of bound water ($Zn/6H_2O$: 15.73, PAM-$Zn/5H_2O$: 5.63, PAM-$Zn/4H_2O$: 5.42, PAM-$Zn/3H_2O$: 4.52, PAM-$Zn/2H_2O$: 3.07, PAM-Zn/H_2O: 1.84). In fact, it is hard to predict the precise coordination number of polymer chains and Zn^{2+} ions. Therefore, we simplified the structure model to describe the solvation environment in the hydrogel electrolyte, in which, per Zn^{2+} ion is interacted with one amide group in the polymer chain. This shows that the presence of PMC makes the adsorption of H_2O and Zn^{2+} weakened, and PMC has a

stronger desolvation ability. From this model, it is found that the most stable form exists in the form of PAM-Zn/5H_2O. Figure 4e is a molecular model simulation diagram of PAM-Zn/5H_2O.

Based on the above characterization results and analysis, it can be summarized the principle of Zn exfoliation/deposition in PMC and $ZnSO_4$. Because of in the $ZnSO_4$ aqueous electrolyte, $[Zn(H_2O)_6]^{2+}$ requires huge energy to desolvate the sheath, resulting in a local pH increase.[49, 50] And SO_4^{2-} ions will freely move to the surface of the zinc foil to produce by-reactions and generate a mass of by-products.[56] These by-products accumulate on the surface of the zinc foil, causing polarization to increase. The freely moving Zn^{2+} tends to deposit on the tip of the zinc foil surface under the applied voltage. Moreover, the uneven interfacial electric field and ion concentration result in uneven nucleation. Eventually leads to the formation and growth of dendrites.[14] In the PMC gel electrolyte, on the one hand, Zn^{2+} is bonded to the strongly polar amide group, and a part of the solvation sheath is removed in advance, which greatly reduces the desolvation energy of Zn^{2+} during deposition; On the other hand, a large number of amide groups in PMC hydrogel can guide Zn^{2+} to deposit in a highly preferred orientation. These positive effects make the zinc anode deposition uniform and dense during the cycle. (Figure 4f)

Zn/V_2O_5 battery cycle performance and flexible battery mechanical performance

Then, we investigated the application of PMC hydrogel electrolytes in Zn/V_2O_5 batteries and flexible batteries. Here we choose $V_2O_5 \cdot 1.6\ H_2O$ as the cathode material. According to Liu's work[57], $V_2O_5 \cdot 1.6\ H_2O$ was synthesized by hydrothermal method, and the synthesized material was characterized by TEM and XRD to study its structure. The TEM image (Figure S14) shows that the interplanar spacing of the synthesized material is 0.195 nm, which corresponds to the (006) crystal plane of $V_2O_5 \cdot 1.6\ H_2O$. The XRD pattern (Figure S15) shows that the diffraction peak of the synthesized material can correspond to the standard peak of $V_2O_5 \cdot 1.6\ H_2O$. These characterizations all indicate that the synthesized material is $V_2O_5 \cdot 1.6\ H_2O$. The synthesized material was made into a positive electrode, PMC hydrogel and 2.0 M $ZnSO_4$ aqueous solution were used as the electrolyte, and zinc foil was used as the anode to assemble a Zn/V_2O_5 full battery. The assembled battery is cycled at a current density of 1.0 A g^{-1}, as shown in the Figure5a, the initial specific capacity of the battery assembled with PMC hydrogel electrolyte is 380.74 mAh g^{-1}, and after 500 cycles, it shows a higher capacity retention rate (71.1%). The initial specific capacity of the battery assembled with 2.0 M $ZnSO_4$ aqueous electrolyte is 360.22 mAh g^{-1}, and the capacity decays relatively quickly in the first 30 cycles. After 500 cycles, the capacity retention rate is only 42.2%. Moreover, Figure 5b shows that the Zn/V_2O_5 battery assembled with PMC hydrogel electrolyte can maintain a relatively stable charge and discharge platform. It can be seen from Figure 5c that the battery using PMC hydrogel electrolyte exhibits good rate performance (0.1 A g^{-1} to 2.0 A g^{-1}). It shows a high initial capacity of 405.5 mAh g^{-1} at a current density of 0.1 A g-1, and

provides a capacity of 349.9 mAh g^{-1} even at a high current density of 2.0 A g^{-1} (Figure 5d). These results all indicate that PMC hydrogel electrolyte has good application prospects in AZIBs.

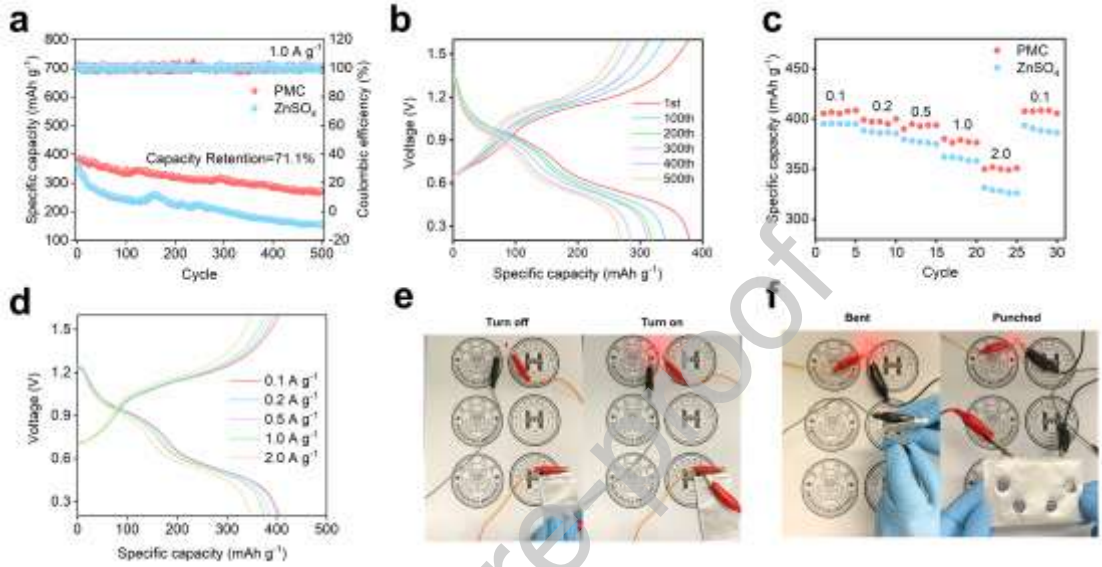

Fig 5. The application of PMC hydrogel electrolyte in Zn/V_2O_5 battery and flexible battery. (a) Cycle performance of Zn/V_2O_5 batteries with different electrolytes (Current density: 1.0 A g^{-1}); (b) Voltage/capacitance diagram of Zn/V_2O_5 batteries assembled with PMC hydrogel electrolyte (Current density: 1.0 A g^{-1}); (c) Rate performance of Zn/V_2O_5 battery assembled by PMC and $ZnSO_4$ (Current density: 0.1-2.0 A g^{-1}); (d) The rate performance of Zn/V_2O_5 battery assembled by PMC hydrogel battery; (e) Zn/V_2O_5 assembled with PMC hydrogel electrolyte the flexible battery lights up the diode; (f) The bending and punching experiment of the Zn/V_2O_5 flexible battery assembled with PMC hydrogel electrolyte.

The better flexibility of PMC hydrogel electrolyte can cope with the mechanical

damage of battery caused by most deformations in daily use, which can extend the life of electronic products and increase the scope of use. In order to verify, we made a flexible battery Zn/PMC/V_2O_5, which can normally supply power to the diode when the battery is energized (Figure 5e, Movie S1). Although the battery was bended from 0 degrees to 180 degrees, it can still normally power the diode (Figure 5f, S16, Movie S2). Furthermore, we conducted a hole-punch test on the flexible battery. After four times of drilling, the flexible battery can still power the diode (Figure 5f, S17), showing great safety and wear resistance.

3. Discussion

In summary, we have successfully synthesized a hydrogel electrolyte PCM using the one-pot method, which has an ionic conductivity of 30.24 mS cm^{-1}. According to the characterization results, the amide group in the PMC hydrogel electrolyte with 3D network can guide the highly preferential orientation of zinc ion deposition, and its bonding with hydrated zinc ion can effectively reduce the desolvation energy. This not only significantly solves the problem of by-products caused by the $ZnSO_4$ aqueous electrolyte, but also the Zn/Zn symmetrical battery assemble using PMC has stable deposition/exfoliation at the current density of 1.0 mA cm^{-2} and the capacity density of 1.0 mAh cm^{-2} for ~5000 h. Meanwhile, the observation under in-situ microscope shows that the PMC helps the Zn^{2+} deposits uniformly and densely. The assembled Zn/Cu and Zn/V_2O_5 batteries show a high degree of reversibility, excellent cycle stability and impressive rate performance. Furthermore, the semi-interpenetrating

network formed by CMC increases the mechanical properties of the hydrogel. The Zn/PMC/V_2O_5 flexible battery prepared by using PMC as the flexible electrolyte has found that the battery has excellent safety and wear resistance. These demonstrated properties make us believe that this work can provide us inspiration, and makes the AZIBs get higher performance and wider application fields.

4. Materials and Methods

Materials

Acrylamide (AM, 99%) and Poly(ethylene glycol) diacrylate (PEGDA, ~600) were purchased in Aladdin. Zinc sulfate heptahydrate ($ZnSO_4 \cdot 7H_2O$, AR) and ammonium persulfate ($(NH_4)_2S_2O_8$, APS, AR) were purchased in Shanghai Hushi. Sodium acrylate (SAA, CP) and 30% hydrogen peroxide (H_2O_2, AR) were purchased from Xilong Science. Polyvinylidene fluoride (PVDF) and carboxymethyl cellulose (CMC) were purchased from Guangzhou Songbai Chemical. Zinc foil (~0.1 mm and ~0.05 mm), copper foil (~0.015 mm) and titanium foil (~0.05 mm) were purchased at Saibo Electrochemical. Vanadium pentoxide (V_2O_5, 99.8%) was purchased from Shang Hai Energy Chemical. Glass fiber (1 mm) was purchased in Whatman. Acetylene black was purchased from Jiuding Chemical. The water used in this experiment is deionized water.

Preparation of Polyacrylamide-poly(ethylene glycol) diacrylate-carboxymethyl Cellulose gel electrolyte (PMC)

At room temperature, 0.865 g AM, 0.0233 g PEGDA, 0.0066 g CMC were added into 6 mL 2.0 M $ZnSO_4$ solution and mixed well, then added 0.48 μL 10% APS solution, shook evenly, poured it into the template, and placed it on a heating plate at 40 °C. After heating for 30 min, it was cooled to room temperature to obtain PMC hydrogel electrolyte.

Preparation of Zinc Polyacrylate- poly(ethylene glycol) diacrylate -carboxymethyl cellulose gel electrolyte (PAC)

At room temperature, 1.144 g SAA, 0.0233 g PEGDA, 0.0066 g CMC were added into 6 mL water and mixed well, then added 0.48 μL 10% APS solution, shook evenly, poured it into the template, and heated it on a 50 °C heating plate for 30 min. After cooling to room temperature, the template was immersed in 2.0 M $ZnSO_4$ solution for 24 hours to make zinc sulfate fully enter the gel, and finally PAC hydrogel electrolyte was obtained.

Preparation of cathode material (V_2O_5·1.6 H_2O)

The material was synthesized by hydrothermal method, 0.3306 g V_2O_5 and 60 mL H_2O were added to the beaker, then 1.5 mL 30% H_2O_2 was added, and the solution turned orange-red after stirring for 30 min. Transfer to a polytetrafluoroethylene autoclave and heat up to 190 °C (30 °C min^{-1}) for 6 hours. The solution after the reaction was filtered with suction and washed with deionized water three times. The filter cake was taken and dried in an oven at 80 °C for 24 h to obtain the product.[57]

Button battery assembly

The CR2016 battery was assembled in an indoor air environment and passed the battery test system (LAND CT2001A, Wuhan, China) for electrochemical performance testing. The anode is zinc foil (~0.1 mm). $V_2O_5 \cdot 1.6\ H_2O$ material, acetylene black and PVDF were mixed in a ratio of 7:2:1 with NMP as a solvent, and the slurry was smeared on the Ti foil to prepare the cathode. The coated cathode needed to be dried in a vacuum oven at 80 °C for more than 12 hours. The mass of the cathode electrode is approximately 1.0 mg cm^{-2}. The PMC and PAC hydrogel are cut into 18 mm diameter thin slices as electrolyte, and the battery assembled with 2.0 M $ZnSO_4$ electrolyte will use 18 mm glass fiber as electrolyte and separator.

Flexible battery assembly

The flexible battery was also assembled in an indoor air environment, and the anode was zinc foil (~0.05 mm). The preparation of the cathode was the same as in section 2.5. The anode, cathode and PMC hydrogel were all cut into sizes of 50*80 mm and 30*80 mm, and the assembled battery was encapsulated in an aluminum-plastic film to obtain a complete flexible battery.

Characterization

Field emission scanning electron microscope (SEM, Zeiss) was used to analyze the surface morphology and X-ray energy spectrum (EDS) of the sample. Projection

electron microscope (TEM, FEI Tecnai F30) was used to observe the morphology of $V_2O_5 \cdot 1.6\ H_2O$. Fourier transform infrared spectrometer (FTIR, Nicolet iS5, Themor Electro Co., USA) was used for the analysis of PMC structure. X-ray diffraction (XRD) and grazing incidence X-ray diffraction (GIXRD) (Rigaku Ultima IV) were used to analyze the composition of the material and the analysis of the deposition form on the surface of the zinc foil. The electrochemical workstation (CHI 730i) was used to perform cyclic voltammetry (CV, scanning speed of 0.5 mV s^{-1}), alternating current impedance spectroscopy (EIS, measurement using conductivity electrodes, measuring range from 100k Hz to 0.1 Hz) and The Tafel curve (measurement using a three-electrode system, using zinc foil as the working electrode and counter electrode, respectively, the saturated calomel electrode (SEC) as the reference electrode, and the scanning speed was 0.1 mV s^{-1}). Optical microscope (BX43, Olympus) was used for in-situ imaging of the deposition form of zinc on the surface of zinc foil under different electrolytes. Electronic tensile testing machine (TSL-1002) was used to test the tensile strength of PMC gel electrolyte.

Ionic conductivity was calculated by the following formula:

$$\sigma = \frac{K}{R} \quad (5)$$

Where σ was the ionic conductivity, K was the cell constant (0.998 cm^{-1}), and R was the bulk resistance.

Credit Author Statement

Pengxiang Lin: Conceptualization, Methodology, Investigation, Experiment, Writing

- original draft; **Jianlong Cong:** design of experiments, partial work of the study; **Jiyang Li** and **Minghao Zhang:** discussion of involved mechanism; **Pengbin Lai:** DFT calculation; **Jing Zeng:** Supervision; **Yang Yang** and **Jinbao Zhao:** Writing - review & editing.

Declaration of Competing Interest

The authors declare that they have no known competing financial interests or personal relationships that could have appeared to influence the work reported in this paper.

Acknowledgements

This research was supported by the National Natural Science Foun- dation of China (Grant Numbers 21875198, 22005257 and 22109030), Natural Science Foundation of Fujian Province of China (No. 2020J05009) and Key R&D Program of Yunnan Province (No. 202103AA080019).

References

[1] X. Feng, D. Ren, X. He, M. Ouyang, Mitigating thermal runaway of lithium-ion batteries, Joule 4(4) (2020) 743-770. https://doi.org/10.1016/j.joule.2020.02.010.

[2] F. Wu, J. Maier, Y. Yu, Guidelines and trends for next-generation rechargeable lithium and lithium-ion batteries, Chemical Society Reviews 49(5) (2020) 1569-1614. https://doi.org/10.1039/c7cs00863e.

[3] H. Liu, Z. Zhu, Q. Yan, S. Yu, X. He, Y. Chen, R. Zhang, L. Ma, T. Liu, M. Li, A disordered rock salt anode for fast-charging lithium-ion batteries, Nature 585(7823) (2020) 63-67. https://doi.org/10.1038/s41586-020-2637-6.

[4] M. Li, J. Lu, Z. Chen, K. Amine, 30 years of lithium-ion batteries, Advanced Materials 30(33) (2018) 1800561. https://doi.org/10.1002/adma.201800561.

[5] J.F. Parker, C.N. Chervin, I.R. Pala, M. Machler, M.F. Burz, J.W. Long, D.R. Rolison, Rechargeable nickel–3D zinc batteries: An energy-dense, safer alternative to lithium-ion, Science 356(6336) (2017) 415-418. https://doi.org/10.1126/science.aak9991.

[6] Q. Yang, Q. Li, Z. Liu, D. Wang, Y. Guo, X. Li, Y. Tang, H. Li, B. Dong, C. Zhi, Dendrites in Zn‐Based Batteries, Advanced Materials 32(48) (2020) 2001854. https://doi.org/10.1002/adma.202001854.

[7] J. Zheng, Q. Zhao, T. Tang, J. Yin, C.D. Quilty, G.D. Renderos, X. Liu, Y. Deng, L. Wang, D.C. Bock, Reversible epitaxial electrodeposition of metals in battery anodes, Science 366(6465) (2019) 645-648. https://doi.org/10.1126/science.aax6873.

[8] Q. Zhang, J. Luan, Y. Tang, X. Ji, H.Y. Wang, Interfacial design of dendrite-free zinc anodes for aqueous zinc-ion batteries, Angew Chem Int Ed Engl 59(32) (2020) 13180-13191. https://doi.org/10.1002/anie.202000162.

[9] J. Shin, J. Lee, Y. Park, J.W. Choi, Aqueous zinc ion batteries: focus on zinc metal anodes, Chem Sci 11(8) (2020) 2028-2044. https://doi.org/10.1039/d0sc00022a.

[10] Y. Cui, Q. Zhao, X. Wu, Z. Wang, R. Qin, Y. Wang, M. Liu, Y. Song, G. Qian, Z. Song, L. Yang, F. Pan, Quasi-solid single Zn-ion conductor with high conductivity enabling dendrite-free Zn metal anode, Energy Storage Materials 27 (2020) 1-8. https://doi.org/10.1016/j.ensm.2020.01.003.

[11] Q. Zhang, J. Luan, X. Huang, Q. Wang, D. Sun, Y. Tang, X. Ji, H. Wang, Revealing the role of crystal orientation of protective layers for stable zinc anode, Nat Commun 11(1) (2020) 3961. https://doi.org/10.1038/s41467-020-17752-x.

[12] Y. Tang, C. Liu, H. Zhu, X. Xie, J. Gao, C. Deng, M. Han, S. Liang, J. Zhou, Ion-confinement effect enabled by gel electrolyte for highly reversible dendrite-free zinc metal anode, Energy Storage Materials 27 (2020) 109-116. https://doi.org/10.1016/j.ensm.2020.01.023.

[13] N. Zhang, X. Chen, M. Yu, Z. Niu, F. Cheng, J. Chen, Materials chemistry for

rechargeable zinc-ion batteries, Chem Soc Rev 49 (2020) 4203-4219. https://doi.org/10.1039/c9cs00349e.

[14] L. Hu, P. Xiao, L. Xue, H. Li, T. Zhai, The rising zinc anodes for high-energy aqueous batteries, EnergyChem 3(2) (2021) 100052. https://doi.org/10.1016/j.enchem.2021.100052.

[15] S.-B. Wang, Q. Ran, R.-Q. Yao, H. Shi, Z. Wen, M. Zhao, X.-Y. Lang, Q. Jiang, Lamella-nanostructured eutectic zinc–aluminum alloys as reversible and dendrite-free anodes for aqueous rechargeable batteries, Nature communications 11(1) (2020) 1-9. https://doi.org/10.1038/s41467-020-15478-4.

[16] H. Tian, Z. Li, G. Feng, Z. Yang, D. Fox, M. Wang, H. Zhou, L. Zhai, A. Kushima, Y. Du, Stable, high-performance, dendrite-free, seawater-based aqueous batteries, Nature Communications 12(1) (2021) 1-12. https://doi.org/10.1038/s41467-020-20334-6.

[17] Z. Zhao, J. Zhao, Z. Hu, J. Li, J. Li, Y. Zhang, C. Wang, G. Cui, Long-life and deeply rechargeable aqueous Zn anodes enabled by a multifunctional brightener-inspired interphase, Energy & Environmental Science 12(6) (2019) 1938-1949. https://doi.org/10.1039/c9ee00596j.

[18] Y. Yang, C. Liu, Z. Lv, H. Yang, Y. Zhang, M. Ye, L. Chen, J. Zhao, C.C. Li, Synergistic Manipulation of Zn(2+) Ion Flux and Desolvation Effect Enabled by Anodic Growth of a 3D ZnF2 Matrix for Long-Lifespan and Dendrite-Free Zn Metal Anodes, Adv Mater (2021) 2007388. https://doi.org/10.1002/adma.202007388.

[19] B. Li, J. Xue, C. Han, N. Liu, K. Ma, R. Zhang, X. Wu, L. Dai, L. Wang, Z. He, A hafnium oxide-coated dendrite-free zinc anode for rechargeable aqueous zinc-ion batteries, Journal of Colloid and Interface Science 599 (2021) 467-475. https://doi.org/10.1016/j.jcis.2021.04.113.

[20] Q. Zhang, J. Luan, L. Fu, S. Wu, Y. Tang, X. Ji, H. Wang, The Three-Dimensional Dendrite-Free Zinc Anode on a Copper Mesh with a Zinc-Oriented Polyacrylamide Electrolyte Additive, Angew Chem Int Ed Engl 58(44) (2019) 15841-15847. https://doi.org/10.1002/anie.201907830.

[21] X. Guo, Z. Zhang, J. Li, N. Luo, G.-L. Chai, T.S. Miller, F. Lai, P. Shearing,

D.J.L. Brett, D. Han, Z. Weng, G. He, I.P. Parkin, Alleviation of Dendrite Formation on Zinc Anodes via Electrolyte Additives, ACS Energy Letters (2021) 395-403. https://doi.org/10.1021/acsenergylett.0c02371.

[22] A. Naveed, H. Yang, J. Yang, Y. Nuli, J. Wang, Highly reversible and rechargeable safe Zn batteries based on a triethyl phosphate electrolyte, Angewandte Chemie International Edition 58(9) (2019) 2760-2764. https://doi.org/10.1002/anie.201813223.

[23] H. Yang, Z. Chang, Y. Qiao, H. Deng, X. Mu, P. He, H. Zhou, Constructing a super-saturated electrolyte front surface for stable rechargeable aqueous zinc batteries, Angewandte Chemie International Edition 59(24) (2020) 9377-9381. https://doi.org/10.1002/anie.202001844.

[24] J. Cong, X. Shen, Z. Wen, X. Wang, L. Peng, J. Zeng, J. Zhao, Ultra-stable and highly reversible aqueous zinc metal anodes with high preferred orientation deposition achieved by a polyanionic hydrogel electrolyte, Energy Storage Materials 35 (2021) 586-594. https://doi.org/10.1016/j.ensm.2020.11.041.

[25] C. Li, X. Xie, H. Liu, P. Wang, C. Deng, B. Lu, J. Zhou, S. Liang, Integrated 'all-in-one'strategy to stabilize zinc anodes for high-performance zinc-ion batteries, National science review 9(3) (2022) nwab177. https://doi.org/10.1093/nsr/nwab177.

[26] X. Xie, H. Fu, Y. Fang, B. Lu, J. Zhou, S. Liang, Manipulating Ion Concentration to Boost Two-Electron Mn4+/Mn2+ Redox Kinetics through a Colloid Electrolyte for High-Capacity Zinc Batteries, Advanced Energy Materials 12(5) (2022) 2102393. https://doi.org/10.1002/aenm.202102393.

[27] Y. Huang, Z. Li, Z. Pei, Z. Liu, H. Li, M. Zhu, J. Fan, Q. Dai, M. Zhang, L. Dai, Solid-state rechargeable Zn//NiCo and Zn–air batteries with ultralong lifetime and high capacity: the role of a sodium polyacrylate hydrogel electrolyte, Advanced Energy Materials 8(31) (2018) 1802288. https://doi.org/10.1002/aenm.201802288.

[28] F. Mo, Z. Chen, G. Liang, D. Wang, Y. Zhao, H. Li, B. Dong, C. Zhi, Zwitterionic sulfobetaine hydrogel electrolyte building separated positive/negative ion

migration channels for aqueous Zn-MnO2 batteries with superior rate capabilities, Advanced Energy Materials 10(16) (2020) 2000035. https://doi.org/10.1002/aenm.202000035.

[29] C. Li, X. Xie, S. Liang, J. Zhou, Issues and future perspective on zinc metal anode for rechargeable aqueous zinc-ion batteries, Energy & Environmental Materials 3(2) (2020) 146-159. https://doi.org/10.1002/eem2.12067.

[30] H. Li, C. Han, Y. Huang, Y. Huang, M. Zhu, Z. Pei, Q. Xue, An extremely safe and wearable solid-state zinc ion battery based on a hierarchical structured polymer electrolyte, Energy Environ Sci 11 (2018) 941-951. https://doi.org/10.1039/C7EE03232C.

[31] P. Yu, Y. Zeng, H. Zhang, M. Yu, Y. Tong, X. Lu, Flexible Zn-ion batteries: recent progresses and challenges, Small 15(7) (2019) 1804760. https://doi.org/10.1002/smll.201804760.

[32] H. Dong, J. Li, J. Guo, F. Lai, F. Zhao, Y. Jiao, D.J. Brett, T. Liu, G. He, I.P. Parkin, Insights on Flexible Zinc - Ion Batteries from Lab Research to Commercialization, Advanced Materials 33(20) (2021) 2007548. https://doi.org/10.1002/adma.202007548.

[33] T. Ye, J. Wang, Y. Jiao, L. Li, E. He, L. Wang, Y. Li, Y. Yun, D. Li, J. Lu, A Tissue-Like Soft All-Hydrogel Battery, Advanced Materials 34(4) (2022) 2105120. https://doi.org/10.1002/adma.202105120.

[34] Z. Chen, X. Li, D. Wang, Q. Yang, L. Ma, Z. Huang, G. Liang, A. Chen, Y. Guo, B. Dong, Grafted MXene/polymer electrolyte for high performance solid zinc batteries with enhanced shelf life at low/high temperatures, Energy & Environmental Science 14(6) (2021) 3492-3501. https://doi.org/10.1039/d1ee00409c.

[35] B. Wang, J. Li, C. Hou, Q. Zhang, Y. Li, H. Wang, Stable hydrogel electrolytes for flexible and submarine-use Zn-ion batteries, ACS Applied Materials & Interfaces 12(41) (2020) 46005-46014. https://doi.org/10.1021/acsami.0c12313.

[36] D. Yuan, J. Zhao, H. Ren, Y. Chen, R. Chua, E.T.J. Jie, Y. Cai, E. Edison, W.J.

Manalastas, M.W. Wong, M. Srinivasan, Anion texturing towards dendrite-free Zn anode for aqueous rechargeable battery, Angew Chem Int Ed Engl 60(13) (2020) 7213-7219. https://doi.org/10.1002/anie.202015488.

[37] M. Zhou, S. Guo, J. Li, X. Luo, Z. Liu, T. Zhang, X. Cao, M. Long, B. Lu, A. Pan, G. Fang, J. Zhou, S. Liang, Surface-Preferred Crystal Plane for a Stable and Reversible Zinc Anode, Adv Mater (2021) 2100187. https://doi.org/10.1002/adma.202100187.

[38] C. Yang, H. Huang, S. Fan, C. Yang, Y. Chen, B. Yu, W. Li, J. Liao, A Novel Dual-Crosslinked Functional Hydrogel Activated by POSS for Accelerating Wound Healing, Advanced Materials Technologies 6(4) (2021) 2001012. https://doi.org/10.1002/admt.202001012.

[39] H. Wang, Q. Wang, X. Cao, Y. He, K. Wu, J. Yang, H. Zhou, W. Liu, X. Sun, Thiol-branched solid polymer electrolyte featuring high strength, toughness, and lithium ionic conductivity for lithium-metal batteries, Advanced Materials 32(37) (2020) 2001259. https://doi.org/10.1002/adma.202001259.

[40] Y. Mao, H. Ren, J. Zhang, T. Luo, N. Liu, B. Wang, S. Le, N. Zhang, Modifying hydrogel electrolyte to induce zinc deposition for dendrite-free zinc metal anode, Electrochimica Acta 393 (2021) 139094. https://doi.org/10.1016/j.electacta.2021.139094.

[41] M. Chen, J. Chen, W. Zhou, X. Han, Y. Yao, C.P. Wong, Realizing an All-Round Hydrogel Electrolyte toward Environmentally Adaptive Dendrite-Free Aqueous Zn-MnO2 Batteries, Adv Mater 33(9) (2021) 2007559. https://doi.org/10.1002/adma.202007559.

[42] X. Shen, L. Peng, R. Li, H. Li, X. Wang, B. Huang, D. Wu, P. Zhang, J. Zhao, Semi - Interpenetrating Network - Structured Single - Ion Conduction Polymer Electrolyte for Lithium-Ion Batteries, ChemElectroChem 6(17) (2019) 4483-4490. https://doi.org/10.1002/celc.201901045.

[43] T. Zhu, Y. Cheng, C. Cao, J. Mao, L. Li, J. Huang, S. Gao, X. Dong, Z. Chen, Y.

Lai, A semi-interpenetrating network ionic hydrogel for strain sensing with high sensitivity, large strain range, and stable cycle performance, Chemical Engineering Journal 385 (2020) 123912. https://doi.org/10.1016/j.cej.2019.123912.

[44] E. Onyiriuka, Zinc phosphate glass surfaces studied by XPS, Journal of non-crystalline solids 163(3) (1993) 268-273. https://doi.org/10.1016/0022-3093(93)91304-L.

[45] W. Xu, C. Liu, Q. Wu, W. Xie, W.-Y. Kim, S.-Y. Lee, J. Gwon, A stretchable solid-state zinc ion battery based on a cellulose nanofiber–polyacrylamide hydrogel electrolyte and a Mg 0.23 V 2 O 5· 1.0 H 2 O cathode, Journal of Materials Chemistry A 8(35) (2020) 18327-18337. https://doi.org/10.1039/D0TA06467J.

[46] M. Chen, J. Chen, W. Zhou, J. Xu, C.-P. Wong, High-performance flexible and self-healable quasi-solid-state zinc-ion hybrid supercapacitor based on borax-crosslinked polyvinyl alcohol/nanocellulose hydrogel electrolyte, Journal of Materials Chemistry A 7(46) (2019) 26524-26532. https://doi.org/10.1039/c9ta10944g.

[47] L. Han, H. Huang, X. Fu, J. Li, Z. Yang, X. Liu, L. Pan, M. Xu, A flexible, high-voltage and safe zwitterionic natural polymer hydrogel electrolyte for high-energy-density zinc-ion hybrid supercapacitor, Chemical Engineering Journal 392 (2020) 123733. https://doi.org/10.1016/j.cej.2019.123733.

[48] W. Yang, X. Du, J. Zhao, Z. Chen, J. Li, J. Xie, Y. Zhang, Z. Cui, Q. Kong, Z. Zhao, Hydrated eutectic electrolytes with ligand-oriented solvation shells for long-cycling zinc-organic batteries, Joule 4(7) (2020) 1557-1574. https://doi.org/10.1016/j.joule.2020.05.018.

[49] Y. Yang, C. Liu, Z. Lv, H. Yang, Y. Zhang, M. Ye, L. Chen, J. Zhao, C.C. Li, Synergistic Manipulation of Zn(2+) Ion Flux and Desolvation Effect Enabled by Anodic Growth of a 3D ZnF2 Matrix for Long-Lifespan and Dendrite-Free Zn Metal Anodes, Adv Mater 33(11) (2021) 2007388. https://doi.org/10.1002/adma.202007388.

[50] H. Yang, Y. Qiao, Z. Chang, H. Deng, X. Zhu, R. Zhu, Z. Xiong, P. He, H. Zhou, Reducing Water Activity by Zeolite Molecular Sieve Membrane for Long-Life Rechargeable Zinc Battery, Adv Mater 33(38) (2021) 2102415.

https://doi.org/10.1002/adma.202102415.

[51] J.Y. Kim, G. Liu, G.Y. Shim, H. Kim, J.K. Lee, Functionalized Zn@ ZnO Hexagonal Pyramid Array for Dendrite-Free and Ultrastable Zinc Metal Anodes, Advanced Functional Materials 30(36) (2020) 2004210. https://doi.org/10.1002/adfm.202004210.

[52] O. Borodin, J. Self, K.A. Persson, C. Wang, K. Xu, Uncharted waters: super-concentrated electrolytes, Joule 4(1) (2020) 69-100. https://doi.org/10.1016/j.joule.2019.12.007.

[53] G.G. Cameron, M.D. Ingram, G.A. Sorrie, The mechanism of conductivity of liquid polymer electrolytes, Journal of the Chemical Society, Faraday Transactions 1: Physical Chemistry in Condensed Phases 83(11) (1987) 3345-3353. https://doi.org/10.1039/F19878303345.

[54] E. Quartarone, P. Mustarelli, Electrolytes for solid-state lithium rechargeable batteries: recent advances and perspectives, Chemical Society Reviews 40(5) (2011) 2525-2540. https://doi.org/10.1039/c0cs00081g.

[55] R. Bakar, S. Darvishi, T. Li, M. Han, U. Aydemir, S. Nizamoglu, K. Hong, E. Senses, Effect of Polymer Topology on Microstructure, Segmental Dynamics, and Ionic Conductivity in PEO/PMMA-Based Solid Polymer Electrolytes, ACS Applied Polymer Materials 4(1) (2021) 179–190. https://doi.org/10.1021/acsapm.1c01178.

[56] C. Liu, X. Xie, B. Lu, J. Zhou, S. Liang, Electrolyte Strategies toward Better Zinc-Ion Batteries, ACS Energy Letters 6(3) (2021) 1015-1033. https://doi.org/10.1021/acsenergylett.0c02684.

[57] S. Liu, H. Zhu, B. Zhang, G. Li, H. Zhu, Y. Ren, H. Geng, Y. Yang, Q. Liu, C.C. Li, Tuning the Kinetics of Zinc-Ion Insertion/Extraction in V2 O5 by In Situ Polyaniline Intercalation Enables Improved Aqueous Zinc-Ion Storage Performance, Adv Mater 32(26) (2020) 2001113. https://doi.org/10.1002/adma.202001113.

Pengxiang Lin: conceptualization, methodology, investigation, experiment, writing-original draft preparation; **Jianlong Cong:** design of experiments, partial work of the study; **Jiyang Li** and **Minghao Zhang:** discussion of involved mechanism; **Pengbin Lai:** DFT calculation; **Jing Zeng:** supervision; **Yang Yang** and **Jinbao Zhao:** reviewing and editing.

Declaration of interests

☒ The authors declare that they have no known competing financial interests or personal relationships that could have appeared to influence the work reported in this paper.

☐The authors declare the following financial interests/personal relationships which may be considered as potential competing interests: